Journal of Oceanography, Vol. 62, pp. 133 to 142, 2006

Mechanism for Enhanced Diffusivity in the Deep-Sea Perpetual Salt Fountain

XINRONG ZHANG[1]*, SHIGENAO MARUYAMA[1], KOUTARO TSUBAKI[1], SEIGO SAKAI[2] and MASUD BEHNIA[3]

[1]*Institute of Fluid Science, Tohoku University, Katahira, Aoba-ku, Sendai 980-8577, Japan*
[2]*Graduate School of Engineering, Yokohama National University, Tokiwadai, Hodogaya-ku, Yokohama 240-8501, Japan*
[3]*Office of the Dean of Graduate Studies, The University of Sydney, NSW 2006, Australia*

(Received 23 May 2005; in revised form 24 August 2005; accepted 10 November 2005)

The mechanism of enhanced diffusivity occurring in the deep-sea perpetual salt fountain has been investigated experimentally and numerically. Some factors which possibly contribute to the enhanced diffusivity were found to be the pipe oscillation with ocean waves and its baffled wall surface. Field experiments in the ocean (Onagawa Bay of Miyagi, Japan) and numerical simulations were performed to study and confirm the dynamics of the flow and heat transport with enhanced diffusivity occurring in upwelling deep-sea water. The agreement between the field experimental data and the numerical solutions of an oscillating-wall boundary condition imposed on the baffled pipe is encouraging, and it indicates the baffled pipe surface subject to the oscillatory motion leads to the enhanced diffusivity. The buoyancy force and then upwelling velocity can be greatly increased by the enhanced diffusivity. The dominant mechanism is the occurrence of complicated vortices and vortex shedding leading to efficient mixing and enhanced diffusion.

Keywords:
· Deep water,
· upwelling,
· perpetual salt fountain,
· turbulent diffusion,
· tracer,
· Pacific Ocean.

1. Introduction

There are large areas in the middle part of the Pacific Ocean with sufficient sunshine but few nutrients on the surface and very low phytoplankton productivity. The food chain in an ocean starts with phytoplankton, so these areas of low productivity are called an ocean desert, where there is a very poor production of fish and sea plants. But in these same areas, water deeper than 200 m below the sea surface, where no sun light penetrates, contains much more nutrient than the surface water (Takahashi and Iseki, 2000).

Recently, Maruyama *et al*. (2000) proposed "the Laputa project" for ocean farming applications. A number of floating pipes are deployed with buoys in an ocean desert area. The nutrient-rich deep water is upwelled by a mechanism called "the perpetual salt fountain" to the region where the sunlight reaches, where phytoplankton can be cultivated. The increase in phytoplankton will enhance the food chain, so fisheries and sea plant fields will be formed, and eventually a floating "ocean forest" may be realized. The perpetual salt fountain was proposed by Stommel *et al*. (1956), who described the possibility of a permanent upwelling of deep seawater using the differences in temperature and salinity between surface seawater and deep seawater. Figure 1 shows the conceptual principle of the perpetual salt fountain. In the ocean desert regions, the surface layers have higher temperature and salinity than those of the deep water. If a long tube were lowered from the surface to a depth of low salinity water, and the deep seawater were slowly pumped up to the surface through the tube, and then the pump were disconnected, the seawater would continue to flow by itself. This phenomenon occurs because the slow upward motion through the tube allows the water inside it to attain the same temperature as the surrounding water. Its salinity, and hence density, is therefore less than that of its surroundings outside the tube, and hence the entire column of water inside the tube is buoyant with respect to the fluid outside at the same level.

Several artificial methods of drawing up deep seawater are known, such as OTEC (Ocean Thermal Energy Conversion) (Otsuka *et al*., 2000). These methods are expensive to deploy in large areas, and ocean storms

* Corresponding author. E-mail: scho@mail.doshisha.ac.jp

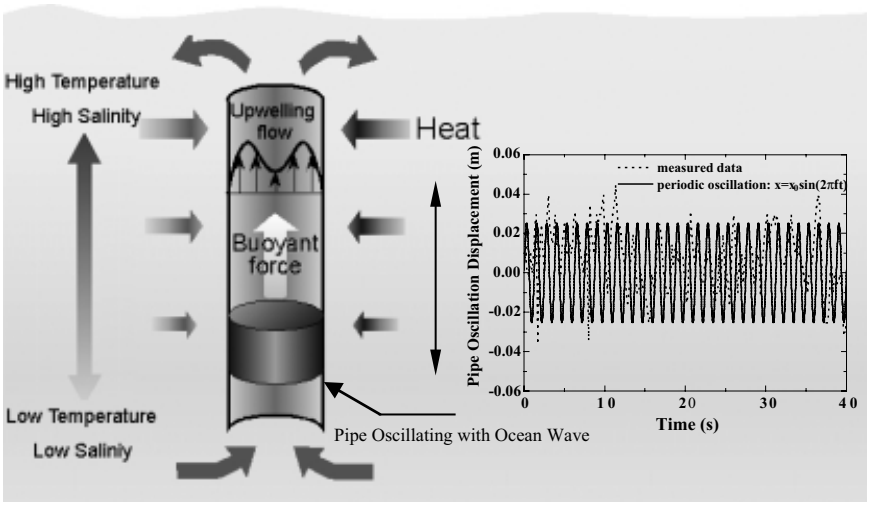

Fig. 1. Conceptual principle of the perpetual salt fountain. Right panel shows variations of pipe oscillation displacement with time. Pipe motion is simplified as a periodic oscillation, in which the oscillation amplitude and frequency represent the average values of the amplitudes and frequencies of the pipe motion.

may destroy the mechanical structure on the sea during long periods of operation. Furthermore, pumped-up cold, deep seawater may sink due to its higher density. But drawing up deep seawater using the perpetual salt fountain means there is no energy input, so it is an easy way to upwell deep seawater in large quantities. In addition, without any mechanical structures except buoys on the ocean surface, the system can be operated for a long time without maintenance. The most important factor is that the upwelled deep seawater is heated during its flow through the pipe and remains on the surface regions (Zhang *et al*., 2004a).

However, after the perpetual salt fountain was proposed, only a simple laboratory experiment demonstrated the principle, and Howard and Stommel failed to measure any flow and velocity using a 1000 m pipe in the ocean, due to the low velocity and strong wave motions (Huppert and Turner, 1981). In August, 2002, actual upwelling velocity was successfully measured at the upper ocean of the Mariana Trench region in the Pacific Ocean (Maruyama *et al*., 2004). A special diffusion method was adopted to measure the low axial velocity in the pipe at a point 15 m below the pipe exit. The velocity was 2.45 mm/s and the vertical (axial) mass diffusion coefficient of the tracer was estimated to be 10^{-5} m^2/s, which is about four orders of magnitude higher than the molecular diffusion coefficient.

Furthermore, a two-dimensional numerical analysis (with stationary smoothed pipe) was developed to predict the upwelling flow and heat transfer occurring in the Mariana Trench experiment (Zhang *et al*., 2004a). Both laminar model and artificial turbulent flow model (the momentum diffusivity and thermal diffusivity in the laminar model are changed into values based on the mass diffusivity measured in the experiment (10^{-5} m^2/s)) are considered in the prediction of the upwelling velocity, temperature and density distributions. The predicted upwelling velocity using the laminar flow model is much lower than the experimental value of 2.45 mm/s. The predicted tracer concentration profile using the molecular diffusivity under the steady-state laminar flow condition does not match the experimental data. The upwelling velocity predicted by the artificial turbulence model produced a value much closer to the experimental one. In addition, the predicted tracer diffusion using the measured mass diffusivity (10^{-5} m^2/s) by the artificial turbulent simulation agrees reasonably well with the measured concentration profile.

All the results support the conclusion that the induced upwelling flow in the Mariana experiment is due to natural convection of turbulent transport with much larger mass diffusion than molecular or laminar diffusion. But the fundamental reasons why the enhanced diffusivity occurs and why its mass diffusion coefficient is very large (about four orders of magnitude higher than the molecular diffusion coefficient) are still not clear, nor is the complex nature of the flow and heat transport of this kind of turbulent convection well understood. Hence, the objectives of the present study are to find the fundamental reasons and attempt to shed some light on the possible mechanisms for this enhanced diffusivity. Numerical simulation with oscillating boundary conditions and deformed

pipe wall surface and ocean experiments have been carried out to achieve the objectives of the paper.

2. Problem Overview

In the ocean experiment, the pipe could not be stationary. At all times it oscillates with the ocean waves. The investigation into the fundamental reasons and mechanisms for the enhanced diffusivity of the Mariana experiment started from an analysis of the effects of an oscillating-wall on the flow and heat transfer in natural convection. Although the pipe oscillation with ocean waves is a kind of random motion, a detailed analysis shows that the motion can be simplified as a periodic (sinusoidal or cosinoidal) oscillation, shown in Fig. 1, in which the oscillation amplitude and frequency represent the average values of the amplitudes and frequencies of the pipe motion, respectively. A numerical study was carried out on natural convection in such a periodically oscillating vertical flat plate heated to a uniform temperature (Zhang *et al*., 2004b). The results show that a twofold increase in space-time averaged Nusselt number is achieved. But a twofold increase in heat transfer rate due to the oscillating-wall is still not high enough to explain how the turbulent transport of the Mariana experiment occurs, with a mass diffusion four orders of magnitude higher than the molecular diffusion.

In the Mariana experiment, a lightweight, flexible pipe made of nylon-reinforced PVC was used. Steel rings were attached every 0.25 m to maintain a circular cross section, and hence the geometry of the pipe wall varies in a periodic manner along the vertical direction. Figure 2 shows the periodic geometry of the pipe employed in the Mariana experiment. Ropes A and B were set along the pipe to maintain the whole pipe upright and also to hold the weight hung at the end of the pipe. Because the rope length is shorter than the pipe surface length, however, the pipe wall is deformed and not totally straight, similar to an arc-shaped wall surface. The wall shape can be simply represented as a baffled pipe surface as shown in Fig. 2, in which the baffle diameter and baffle spacing are measured to be 0.24 m and 0.25 m, respectively. The question here is whether such a deformed pipe under an oscillating-wall condition leads to the enhanced diffusivity occurring in the Mariana experiment.

The baffled channel is one device employed for enhancing heat and mass transfer efficiency in the fields of bioengineering and chemical and industrial engineering. A number of investigations have demonstrated that the baffled channel leads to an enhancement of heat and mass transfer as compared to the corresponding straight-walled channel (Amano, 1985; Nishimura *et al*., 1986; Mackley and Ni, 1991). In contrast there are researchers who have predicted numerically that the presence of baffles in a tube could actually decrease the heat transfer coefficient

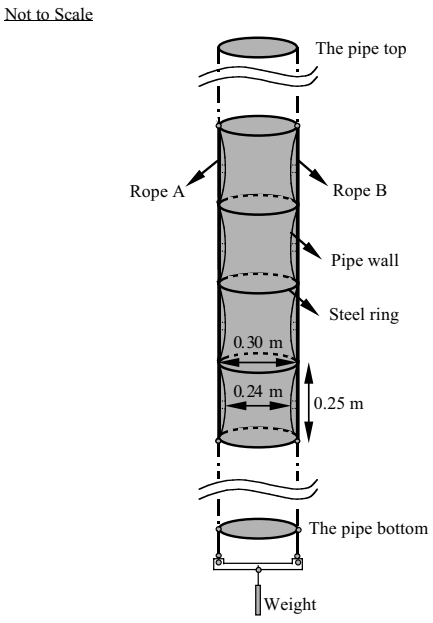

Fig. 2. Diagram of the pipe employed in the Mariana experiment.

(Rowley and Patankar, 1984). In addition, the flow and heat transfer under a combination of oscillatory flow and baffled tube or channel has also already been investigated (Brunold *et al*., 1989; Mackley *et al*., 1990; Howes *et al*., 1991; Mackley and Stonestreet, 1995; Fusegi, 1996; Stephen and Mackley, 2002). These studies all show that both the oscillatory flow condition and baffles need to be present to produce this effect.

However, the previous studies have mainly focused on the detailed analyses of flow structures, such as chaotic flow, bifurcation phenomena and vortex structure. In addition, almost all the previous studies are relevant to forced convection and fluid oscillation in which the tubes remain stationary. During upwelling of the deep seawater, natural convection and tube wall oscillation occur. It appears that no study on the effect of oscillatory deformed wall or baffled wall on the heat and mass transfer have been reported in the open literature. Therefore, the existing studies cannot determine whether the mechanisms controlling the enhanced diffusivity occurring in the Mariana experiment are due to the simplified baffled pipe subject to the wall oscillation condition. The relationship between such an oscillatory baffled pipe and the turbulent transport with a mass diffusion coefficient of about four orders of magnitude higher than the molecular diffusivity, need to be examined in order to gain insight into the mechanisms of the flow and heat transport occurring in the upwelling deep seawater by the perpetual salt fountain in the Mariana experiment.

3. Numerical Simulation Accompanied by Ocean Experiments

3.1 Model formulation

Consider a periodically baffled pipe as shown schematically in Fig. 3. The domain of interest is a two-dimensional axisymmetric one with the pipe diameter d, baffle spacing L and baffle diameter d', repectively. Both the sizes of the computational domain height L_T and width W_T are set large enough to consider the water entering and flowing out of the pipe. The origin of the coordinate system is placed at the pipe centerline. The computational geometry is bounded on the right, top and bottom by solid walls (bottom walls are adiabatic and right wall is set at constant temperature T_w). The top surface is specified as a free surface, which is assumed to be adiabatic. Since the pipe wall is very thin, a zero thickness is assumed in the simulation. The pipe walls are kept at uniform temperature T_w and the salinity out of the pipe at constant S_w. The fluid coming into the pipe has a constant temperature T_∞, constant salinity S_∞ ($S_\infty < S_w$) and average net flow velocity u_n. At time $t < 0$, the pipe wall is assumed to be at rest and the fluid inside the pipe is assumed to be at the temperature T_∞ and the salinity S_∞. For time $t > 0$ the pipe wall starts moving in its own plane. The flow is considered to be unsteady. In the geometry described above, the thermo-physical properties of the working fluid are assumed to be constant except for the density, which is assumed to be a function of the temperature and salinity. The density function can be seen in Zhang *et al*. (2004a).

The governing equations are as follows:

Continuity equation

$$\nabla \cdot (\rho \mathbf{V}) = 0. \tag{1}$$

Momentum equation

$$\frac{\partial(\rho \mathbf{V})}{\partial t} + \nabla \cdot (\rho \mathbf{V}\mathbf{V}) = \mu \nabla^2 \mathbf{V} - \nabla P + \rho \mathbf{g}. \tag{2}$$

Energy equation

$$\frac{\partial(\rho T)}{\partial t} + \nabla \cdot (\rho \mathbf{V} T) = \frac{k}{c_p} \nabla^2 T. \tag{3}$$

Species equation

$$\frac{\partial(\rho S)}{\partial t} + \nabla \cdot (\rho S \mathbf{V}) = \nabla \cdot (\rho D \nabla S), \tag{4}$$

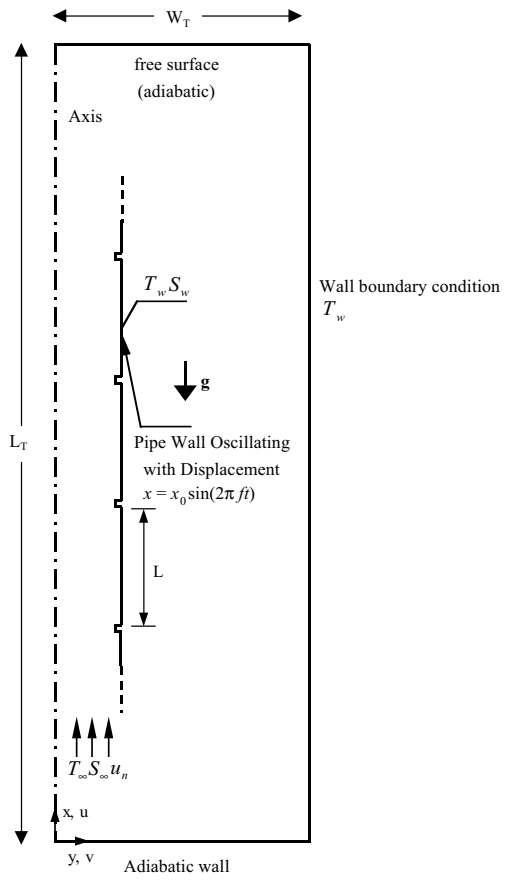

Fig. 3. Baffled pipe geometry with coordinate system.

where ρ, μ, k and c_p are density, dynamic viscosity, thermal conductivity and specific heat for fluid, respectively, $\mathbf{V}$ and $\mathbf{g}$ are dimensional velocity vector and gravity vector, t is time, T is temperature, S is dimensional concentration (salinity), and D is mass diffusivity.

The appropriate boundary conditions considered here are the non-slip conditions on the walls. The mass flow and velocity boundary conditions are respectively specified for the pipe inlet and outlet. The concentration boundary condition on the walls is zero mass flux. The pipe motion is governed by the time-dependent equations, in which the displacement of oscillation and the oscillatory velocity have the form

$$x = x_0 \sin(2\pi f t), \tag{5}$$

$$u = 2\pi f x_0 \cos(2\pi f t), \tag{6}$$

where x_0 and f are the oscillation amplitude and frequency, respectively, and t is time.

An examination of the governing equations and

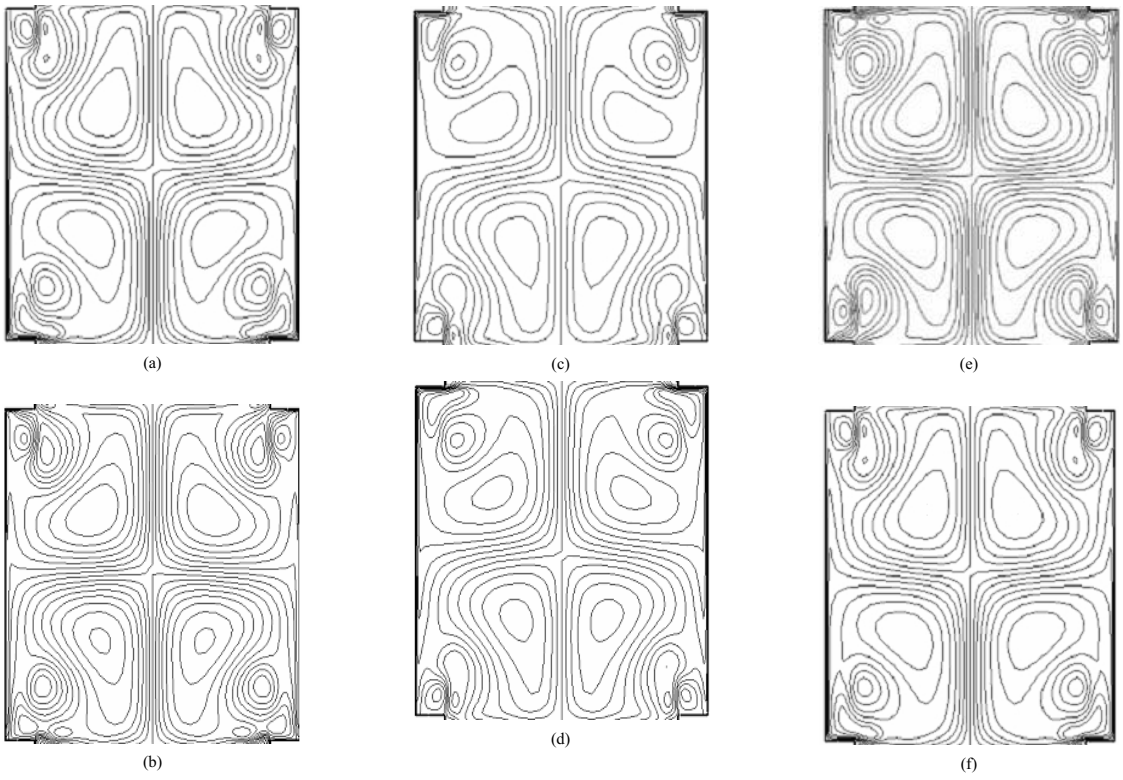

Fig. 4. Time sequence of instantaneous flow patterns in the (x, y)-plane for one oscillation cycle. The net flow Reynolds number Re_n, the oscillatory Reynolds number Re_o, the Strouhal number St and the Stroke ratio Sr are 0, 10726, 0.6 and 0.8 respectively. (a) $t = t_0$ (an integer), (b) $t = t_0 + 0.2$, (c) $t = t_0 + 0.4$, (d) $t = t_0 + 0.6$, (e) $t = t_0 + 0.8$, and (f) $t = t_0 + 1.0$.

boundary conditions shows that four dimensionless groups describe this flow in the present study, namely the net flow Reynolds number, $Re_n = \rho u_n d/\mu$, the oscillatory Reynolds number, $Re_o = 2\pi x_0 f \rho d/\mu$, the Strouhal number, $St = d'/\pi x_0$, which represents a ratio of baffle diameter to oscillation amplitude, and the Stroke ratio $Sr = 2x_0/L$, measuring oscillation amplitude applied to the system expressed as the number of baffle spacing.

In this work, a finite-volume numerical technique based on integration over the control volume was used to solve the coupled governing equations for u, v, T and C. The numerical technique is essentially the same as that used by Zhang *et al.* (2004a) and further details can be found there. A structured, non-uniform grid system was used to solve the discretized equations. The grid was made finer towards the pipe wall in order to model accurately the solution variables with large gradients in the near-wall region and adequately capture solutions under the oscillating-wall conditions. Because of the extremely thin velocity and thermal boundary layers at an oscillating-wall condition, a highly non-uniform grid was deployed. The corresponding grid independence of the results was established by employing various numbers of mesh points, ranging from 20,000 to 60,000. The time step independence of the solutions was tested, and the typical implicit time step used is 0.006 s, which was chosen as the uppermost value on balance of convergence and CPU time. All the computations in this paper were carried out on the SGI Origin2000 workstation in the Advanced Fluid Information Research Center at Tohoku University, Japan.

The formulation of the numerical model above is expected to have the capability to deal reasonably with the flow under an oscillating-wall boundary condition. Therefore, for validation of the proposed numerical model, a moving boundary condition $u = u_0\cos(2\pi ft)$ was used to compare with the exact solutions for the Stokes second problem, in which the flow solutions about a flat wall which executes linear harmonic oscillations parallel to itself are given (Schlichting, 1979). In the geometry described above, air (Pr = 0.7) and water (Pr = 10) were used as comprehensive validation efforts. It was found that the present predictions are in excellent agreement with the Stokes exact solution and therefore the model can be considered to be valid (Zhang *et al.*, 2004b).

3.2 Numerical results and discussion

In the present study, numerical calculations of the mass and heat diffusion were performed for the baffled

pipe under the wall oscillation condition. The geometry studied is based on the baffled pipe employed in the visualization experiment. The oscillating-wall condition used is based on the measured values in an ocean experiment, in which the oscillation amplitude and frequency are obtained as 0.04 m and 0.8 Hz respectively. Here, the flow patterns from the numerical prediction are first given using plots of the instantaneous streamlines. Figure 4 is a time sequence of the streamlines showing fluid motion in the (x, y)-plane under the oscillating-wall condition imposed on the baffled pipe at $\mathrm{Re}_n = 0$, $\mathrm{Re}_o = 15046$, $St = 0.6$ and $Sr = 0.8$. The instantaneous streamlines of phase angle $2\pi ft = 0$, 72, 144, 216, 288 and 360 during one oscillation cycle are respectively shown in Figs. 4 (a)–(f). The kinematics of the flow is important in understanding of mechanisms for mass and heat transport. It can be clearly seen that the two-dimensional unsteady flow caused by the oscillatory condition of the baffled pipe is extremely complex. The flow is symmetric with respect to the pipe centerline and exhibits space symmetry. The flow patterns of Fig. 4 indicate that the flow is fully periodic over one oscillation cycle. This is clear from comparison of Figs. 4(a) and (f). In addition, it is obvious that strong pairs of vortices exist through both the flow regime and the oscillation cycle. Further observation of the flow at successive pipe oscillations indicates that the observed vortex structure is also symmetric and time periodic. Another important feature of this flow is that a periodic eddy shedding is predicted in the flow regime. Efficient mixing appears to have occurred. This mixing is not exclusively in the central part of the pipe but extends well into the inter-baffle region and close to the walls. The basic mechanism of mixing is caused by the baffles and oscillatory pipe, leading to a complex process. We believe that the fluid flow caused by the oscillating-wall condition imposed on the baffled pipe can be a very efficient way of generating well-mixed flows. The strong global mixing suggests that improved heat and mass transport can be achieved when compared with an unbaffled pipe operating under a similar condition.

The flow patterns in Fig. 4 give a clear picture of the potential of this system to yield good mixing and enhance mass and heat transport, so the tracer diffusions under the flow patterns were investigated numerically. From the numerical study, the tracer is injected at the middle position of the pipe and its concentration is obtained numerically at the point one pipe radius away from the injection position. The concentration profiles of the tracer are predicted as a function of time at the monitoring point. In Fig. 5, case (a) presents the concentration profiles obtained in the baffled pipe, where the pipe oscillation is present and the molecular mass diffusion coefficient (10^{-9} m^2/s) is given as the mass diffusivity for the tracer. In this simulation, the equivalent "turbulent diffusion"

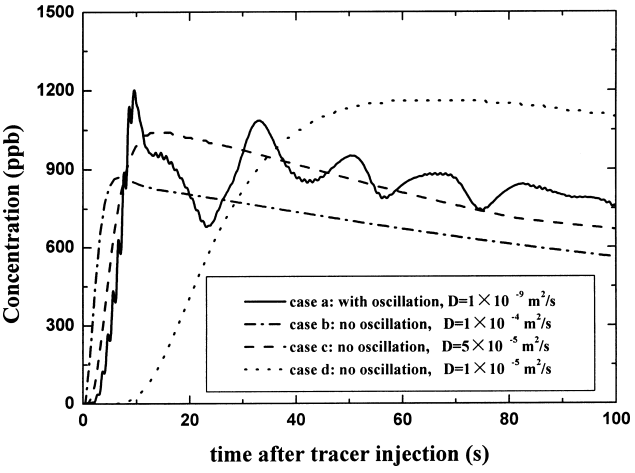

Fig. 5. Relation between elapsed time from tracer injection and its concentration.

coefficients are also used in order to take turbulent mixing effects into account. The cases (b), (c) and (d) are with no oscillation, but an equivalent turbulent mass diffusivity and momentum diffusivity of 10^{-4}, 5×10^{-5} and 10^{-5} m^2/s are assumed, respectively. It is known that there is a very low diffusion and mixing in a smooth-walled pipe without oscillation. In this situation, molecular diffusion is generally the only way in which species within the pipe will become mixed, and the heat and mass transfer rates will consequently be very low. However, it can be seen that the concentration profile predicted using the molecular diffusivity and the oscillating-wall condition imposed on the baffled pipe (case (a)) is in a good agreement with that of the mass diffusivity 5×10^{-5} m^2/s in the absence of the oscillation (case (c)). This simulation quantified the data of mass diffusion coefficient in the periodic baffled-pipe under the oscillating-wall condition. The slow undulation observed in case (a) may be due to the vortices created in the oscillating baffled pipe. Furthermore, the introduction of periodic baffles under the oscillation conditions has the ability to significantly increase the mass diffusivity when compared to an unbaffled pipe without oscillation. This result validates the turbulent mass diffusivity and its order close to the measured coefficient of mass diffusion (10^{-5} m^2/s) in the Mariana experiment (Maruyama *et al.*, 2004).

Furthermore, numerical investigation of the thermal diffusion in the baffled pipe under the oscillating-wall boundary condition was carried out in order to quantify the potential of heat transport under the flow pattern shown in Fig. 4. In this study, the wall temperature is maintained at T_w and at the initial time the fluid temperature is T_∞. We seek a solution of the temperature field inside the pipe as a function of time. Figure 6 shows the

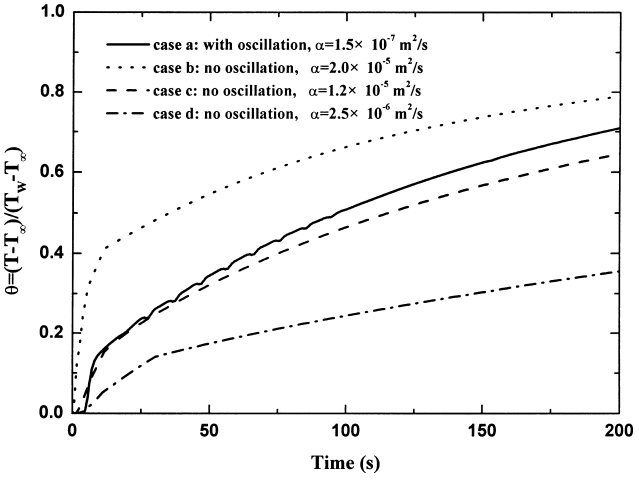

Fig. 6. Relation between elapsed time and computed temperature. θ is dimensionless temperature, and T_w and T_∞ are wall temperature and ambient water temperature.

relation between the elapsed time and the temperature of a point located at the centerline of the pipe. In this figure, there are four different cases for numerical calculations, where case (a) represents the oscillating-wall condition used on the baffled pipe and molecular thermal diffusivity of 1.5×10^{-7} m^2/s given; cases (b), (c) and (d) represent the absence of the oscillating-wall conditions but having an equivalent thermal diffusivity and momentum diffusivity of 2.0×10^{-5}, 1.2×10^{-5} and 2.5×10^{-6} m^2/s, respectively. It is found that the temperature distribution of case (a) falls between the results predicted with the thermal diffusivity of 1.2×10^{-5} m^2/s and 2.0×10^{-5} m^2/s, but close to the profile of 1.2×10^{-5} m^2/s (case (c)). The magnitude of 1.2×10^{-5} is also close to the measured value of the thermal diffusivity (4.5×10^{-6}) in an ocean experiment (Tsubaki, 2003). Furthermore, for the purpose of generalizing the average buoyancy force produced by the salinity difference, based on the area-weighted average of a quantity, the average density inside the pipe $\overline{\rho}$ and the average buoyancy force $\overline{N}$ can be defined as

$$\overline{\rho} = \left(\sum_i \frac{1}{r^2} \int_0^r 2\rho r dy \right) \Big/ i \tag{7}$$

$$\overline{N} = (\rho_o - \overline{\rho}) g. \tag{8}$$

The average buoyancy force is calculated at 8.5 N/m^2 under the oscillating-wall condition used on the baffled pipe and thermal diffusivity 1.5×10^{-7} m^2/s (case (a)). With the absence of the oscillating-wall conditions but with a thermal diffusivity of 2.0×10^{-5} (case (b)), 1.2×10^{-5} (case (c)) and 2.5×10^{-6} m^2/s (case (d)), average buoyancy forces are obtained of 14.2, 8.7 and 2.0 N/m^2, respectively. It can be seen that the buoyancy force of case (a) is also close to that of case (c). The agreement shows that a combination of baffles and oscillating-wall conditions leads to a significant enhancement of the heat transport inside the pipe and therefore buoyancy force increases. We believe that the enhanced heat transport is possibly due to the following mechanisms. First, a simultaneous use of baffles and oscillation conditions will result in strong vortices and vortex shedding, giving a global mixing, not only in the central part of the pipe but also the adjacent part of the wall shown in Fig. 4. Secondly, the thickness of the thermal boundary layer in an oscillating-wall condition is given as (Ozawa and Kawamoto, 1991)

$$\delta_t = \sqrt{\upsilon / \pi f} \,/ \mathrm{Pr}, \tag{9}$$

which implies that the thickness becomes much thinner than that with no oscillatory condition. Consequently, the heat transfer rate can be increased by imposing the wall oscillation conditions. In addition, the introduction of the baffles efficiently interrupt the boundary layer that forms on the pipe wall surface and replace it with fluid from the core, thereby creating a fresh boundary layer that has increased near-wall temperature gradients, so a larger heat/mass transfer rate is achieved. All of the above mechanisms lead to much higher heat transport with the thermal diffusivity of 1.2×10^{-5} in the baffled pipe subjected to the oscillation condition; 100 times larger than the molecular thermal diffusivity.

However, we still have not confirmed whether both the deformed pipe and wall oscillation are the fundamental reasons for the turbulent flow and heat transport occurring during upwelling deep seawater in the Mariana experiment, although the combination of the two factors has the potential of producing the enhanced diffusivity with a magnitude close to that of the Mariana experiment. Furthermore, in order to certify the real mechanism for the onset of turbulent transport of the Mariana experiment, an ocean experiment was carried out in Onagawa Bay of Miyagi, Japan.

3.3 Ocean experiments

In September, 2003, field experiments were carried out in Onagawa Bay of Miyagi, Japan. The experiments were different from the Onagawa experiment reported in Maruyama *et al*. (2004). The Onagawa experiment described in Maruyama *et al*. (2004) was conducted to verify the upwelling velocity measured in the Mariana Trench. A schematic diagram of the experimental set-up is shown in Fig. 7. The same pipe as that employed in the Mariana experiment was used, but its length was 30 m. The top of the pipe was kept above the sea surface in order to avoid

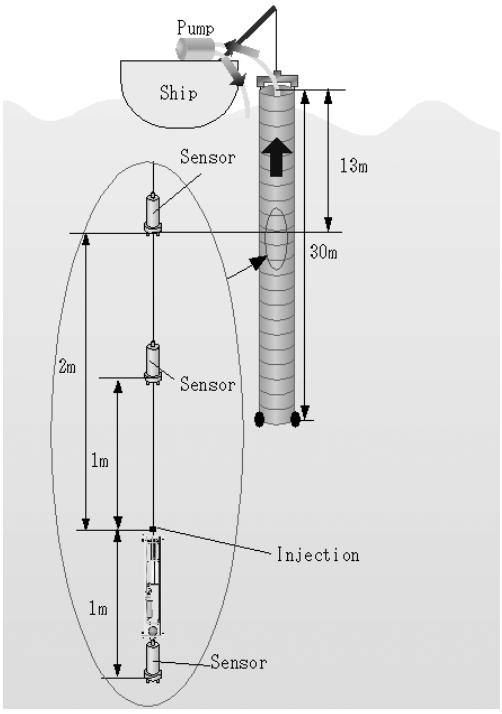

Fig. 7. Diagram of experimental apparatus (Onagawa Bay, Japan, September, 2003).

the influences of natural convection on the flow inside the pipe. Seawater was pumped up in such a way that the average velocity achieved was 2.5 mm/s, equal to the measured value of upwelling velocity in the Mariana experiment. The tracer (Rhodamine WT) was injected into the pipe 13 m below the top of the pipe and at the center of the pipe. Two fluorescent sensors were respectively set 1 m and 2 m above the injector and one sensor was set 1 m below the injector. The detection method and system are based on the previous work reported in Maruyama *et al*. (2004). In this experiment, the pipe motions with ocean waves were also measured and the average values of oscillation amplitudes and frequencies were obtained and found to be 0.025 m and 0.8 Hz, respectively. The measured data were used in the corresponding numerical simulations.

The concentration distributions detected by the sensors are shown in Fig. 8, which also shows numerical predictions by the model described above with Re_n = 561, Re_o = 28211, St = 3.0 and Sr = 0.2. Here, the oscillatory Reynolds number is larger than that of Figs. 4 and 5, so the flow should be a kind of convection with turbulent effects. In the upper panel of Fig. 8, the concentration profiles at 1 m below the injector are almost same as the horizontal axis, because the flow is upward. In Fig. 8, it can be seen that there is good agreement between the ocean experiment data and the calculated concentration profiles using the oscillatory baffled pipe. However, there is a large difference between the measured concentration profiles and the prediction results in an oscillatory smoothed pipe without turbulent mixing.

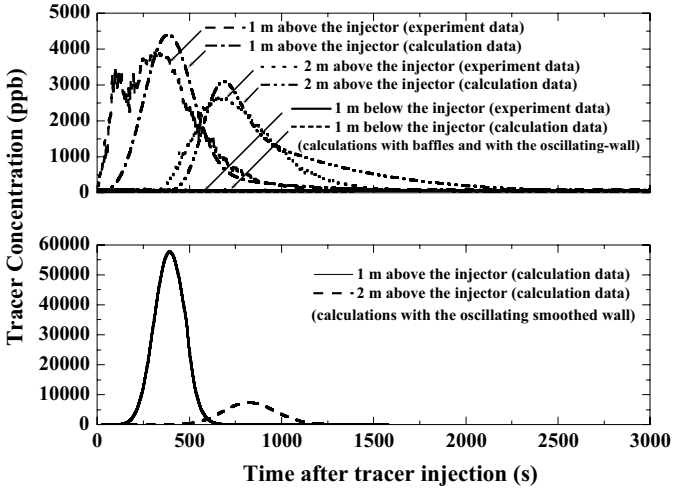

Fig. 8. Comparison between ocean experiment data and numerical predictions. Upper panel shows variations of tracer concentrations obtained in the ocean experiment and numerical simulation with oscillating baffled wall. Good agreements can be seen between the experimental data and the calculated profiles with oscillating baffled pipe. Lower panel shows variations of tracer concentrations obtained in the numerical simulation with oscillating smoothed wall. It can be seen that a large difference exists between the experimental data and the numerical results using oscillating smoothed pipe.

4. Discussion

The agreement above is encouraging and it indicates that the fundamental reasons for the occurrence of the turbulent mass diffusion measured with a magnitude of four orders higher than the molecular diffusion are due to the combination of the deformed pipe and its wall oscillations. It has also been clarified that the dominant mechanisms underlying the turbulent flow and heat transport are the appearances of complex vortices and vortex shedding when the wall oscillation conditions are imposed on the deformed pipe, and the vortex shedding leads to good global mixing and significantly enhances the rate of heat and mass transport.

The power of the perpetual salt fountain comes from the buoyant force, which is largely dependent on the heat transfer process from pipe wall to water inside the pipe. The results of enhanced diffusivities are encouraging, because the enhanced values can greatly increase the heat transfer process (vortices and vortex shedding occur) and buoyant force, and therefore the upwelling flow rate can also be increased. Figure 9 shows the upwelling velocities plotted under the thermal diffusivities, in which the Mariana experiment was simulated numerically with the thermal diffusivity of $a = 10^{-9}$ m^2/s and $a = 10^{-5}$ m^2/s, based on the previously developed model (Zhang *et al.*, 2004a). It can be seen from the figure that the higher thermal diffusivity can greatly enhance the upwelling flow rate. After the flow reaches the steady state, the average upwelling velocity is about 2.23 mm/s ($a = 10^{-9}$ m^2/s) and 28.8 mm/s ($a = 10^{-5}$ m^2/s). But now it is not clear whether the deformed pipe employed in the Mariana experiment is an optimum geometry for the heat and mass transfer that occurs during upwelling deep seawater using the perpetual salt fountain. Other sizes and shape variants are possible, of course, which will lead to better results than those described here. There is clearly a significant scope for further optimization of the geometric design. The mechanisms discussed here indicate a potential for enhancing the heat and mass transport in order to increase the upwelling flow rate in the future.

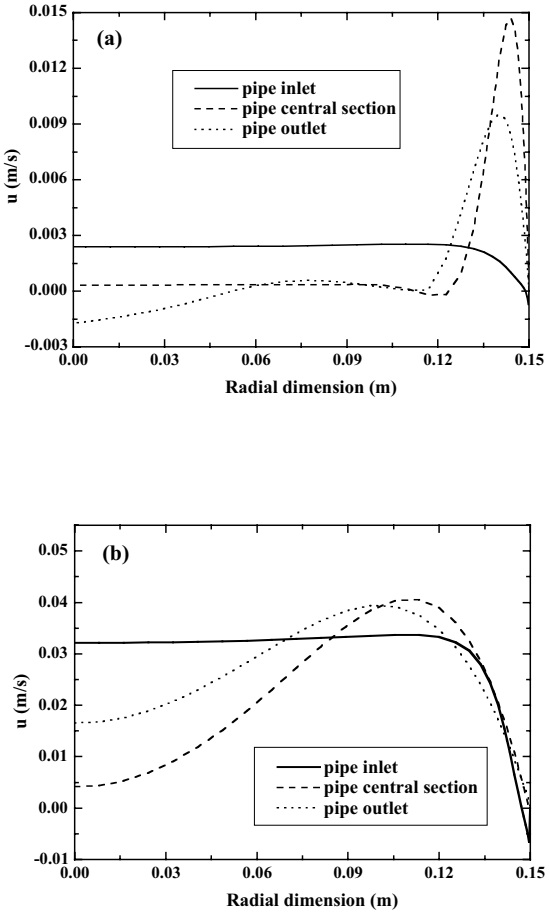

Fig. 9. Upwelling velocities inside the pipe under steady-state flow condition. (a) thermal diffusivity $a = 10^{-9}$ m^2/s; (b) thermal diffusivity $a = 10^{-5}$ m^2/s.

5. Concluding Remarks

The fundamental reasons and mechanisms of the enhanced diffusivity (with a magnitude of four orders higher than the molecular mass diffusivity) occurring when the deep seawater is upwelled using the perpetual salt fountain have been studied experimentally and numerically. The following remarks are based on the results of this study:

(1) The problems of mass and heat diffusion in a baffled pipe under an oscillating-wall condition or in the absence of oscillation were analyzed numerically. The numerical results show that the introduction of baffles into the oscillatory pipe significantly increases the heat/mass diffusion, leading to a kind of turbulent transport with mass diffusivity $D = 5 \times 10^{-5}$ m^2/s and thermal diffusivity $a = 1.2 \times 10^{-5}$ m^2/s, respectively, which are close to the values measured in the ocean experiments. The mechanisms of the enhancements are due to complicated vortices and vortex shedding achieved across the pipe when baffles and oscillation are present.

(2) An ocean experiment has been conducted in Onagawa Bay of Miyagi, Japan. The tracer diffusion data measured are in a good agreement with the numerical results obtained when both pipe oscillation and baffles are present. This agreement confirms that the fundamental reasons for the occurrence of enhanced diffusion in the Mariana experiment are due to the combination of the deformed pipe wall and its oscillations with ocean waves. The enhanced diffusion can be utilized to increase the buoyancy force and velocity of the upwelling flow in the perpetual salt fountain.

Acknowledgements

The calculations were performed using the ORIGIN 2000 (or SX-5) in the Institute of Fluid Science, Tohoku University.

References

Amano, R. S. (1985): A numerical study of laminar and turbulent heat transfer in a periodically corrugated wall channel. *ASME Journal of Heat Transfer*, **107**, 564–569.

Brunold, C. R., J. C. B. Hunns, M. R. Mackley and J. W. Thompson (1989): Experimental observations on flow patterns and energy losses for oscillatory flows in ducts with sharp edges. *Chem. Eng. Sci.*, **44**, 1227–1244.

Fusegi, T. (1996): Mixed convection in periodic open cavities with oscillatory throughflow. *Numerical Heat Transfer, Part A*, **29**, 33–47.

Howes, T., M. R. Mackley and E. P. L. Roberts (1991): The simulation of chaotic mixing and dispersion for periodic flows in baffled channels. *Chem. Eng. Sci.*, **46**, 1669–1677.

Huppert, H. E. and J. S. Turner (1981): Double-diffusive convection. *J. Fluid Mech.*, **106**, 299–329.

Mackley, M. R. and X. Ni (1991): Mixing and dispersion in a baffled tube for steady laminar and pulsative flow in baffled tubes. *Chem. Eng. Sci.*, **45**, 1237–1242.

Mackley, M. R. and P. Stonestreet (1995): Heat transfer and associated energy dissipation for oscillatory flow in baffled tubes. *Chem. Eng. Sci.*, **50**, 2211–2224.

Mackley, M. R., G. M. Tweddle and I. D. Wyatt (1990): Experimental heat transfer measurements for pulsatile flow in baffled tubes. *Chem. Eng. Sci.*, **45**, 1237–1242.

Maruyama, S., M. Ishikawa and K. Taira (2000): Japanese patent #2000-158594.

Maruyama, S., K. Tsubaki, K. Taira and S. Sakai (2004): Cultivation of ocean desert by upwelling deep seawater using perpetual salt fountains. *J. Oceanogr.*, **60**, 563–568.

Nishimura, T., Y. Kajimoto and Y. Kawamura (1986): Mass transfer enhancement in channels with a wavy wall. *J. Chem. Eng. Japan*, **19**, 142–144.

Otsuka, K., A. Bando and H. Inoue (2000): A study on floating-type deep-seawater upwelling system. *OTEC*, **8**, 43–48.

Ozawa, M. and A. Kawamoto (1991): Lumped-parameter modeling of heat transfer enhanced by sinasoidal motion of fluid. *Int. J. Heat Mass Transfer*, **34**, 3083–3095.

Rowley, G. T. and S. V. Patankar (1984): Analysis of laminar flow and heat transfer in tubes with internal circumferential fins. *Int. J. Heat and Mass Transfer*, **27**, 553–560.

Schlichting, H. (1979): *Boundary-Layer Theory*. 7th ed., McGraw-Hill, New York, p. 93–95.

Stephens, G. G. and M. R. Mackley (2002): Heat transfer performance for batch oscillation flow mixing. *Experimental Thermal and Fluid Science*, **25**, 583–594.

Stommel, H., A. B. Arons and D. Blanchard (1956): An ocean curiosity: the perpetual salt fountain. *Deep-Sea Res.*, **3**, 152–153.

Takahashi, M. and K. Iseki (2000): Deep seawater as resource of the 21st century. *Kaiyo*, **22**, 5–10.

Tsubaki, K. (2003): Study on measurement of deep-seawater upwelling by perpetual salt fountain. Master Thesis. Institute of Fluid Science, Tohoku University, Japan, 83 pp.

Zhang, X. R., S. Maruyama, S. Sakai, K. Tsubaki and M. Behnia (2004a): Flow prediction in upwelling deep seawater—the perpetual salt fountain. *Deep-Sea Res. I*, **51**, 1145–1157.

Zhang, X. R., S. Maruyama and S. Sakai (2004b): Numerical investigation of laminar natural convection on a heated vertical plate subjected to a periodic oscillation. *Int. J. Heat and Mass Transfer*, **47**, 4439–4448.